Saturn's Weather-Driven Aurorae Modulate Oscillations in the Magnetic Field and Radio Emissions

M. N. Chowdhury[1], T. S. Stallard[1], K. H. Baines[2,3], G. Provan[1], H. Melin[1], G. J. Hunt[4], L. Moore[5], J. O'Donoghue[6], E. M. Thomas[1], R. Wang[1], S. Miller[7], and S. V. Badman[8]

[1]School of Physics and Astronomy, University of Leicester, Leicester, UK
[2]Jet Propulsion Laboratory, California Institute of Technology, Pasadena, CA, USA
[3]Space Science and Engineering Center, University of Wisconsin-Madison, Madison, WI, USA
[4]Blackett Laboratory, Imperial College London, London, UK
[5]Center for Space Physics, Boston University, Boston, MA, USA
[6]Institute for Space and Astronautical Science, JAXA, Kanagawa, Japan
[7]Department of Physics and Astronomy, University College London, London, UK
[8]Department of Physics, Lancaster University, Lancaster, UK

Key Points:

- Keck-NIRSPEC observations of Saturn's northern H_3^+ infrared auroral emission from 2017 are analysed
- First clear picture of how the ionosphere moves in relation to planetary period currents is provided
- Saturn's measured variable rotation rate is driven by twin-vortex flows in the upper atmosphere

Corresponding author: Nahid Chowdhury, `nahidc14@gmail.com`

Abstract

The Cassini spacecraft revealed that Saturn's magnetic field displayed oscillations at a period originally thought to match the planetary rotation rate but later found not to. One of many proposed theories predicts that a polar twin-cell neutral weather system drives this variation, producing observable differences in flows within Saturn's ionosphere. Here, using spectral observations of auroral H_3^+ emission lines taken by the Keck Observatory's Near Infrared Echelle Spectrograph (Keck-NIRSPEC) in 2017, we derive ion line-of-sight velocity maps after grouping spectra into rotational quadrants matching phases of the planetary magnetic field. We measure 0.5 km s^{-1} wind systems in the ionosphere consistent with predicted neutral twin-vortex flow patterns. These findings demonstrate that neutral winds in Saturn's polar regions cause the rotational period, as determined via the magnetic field, to exhibit differences and time variabilities relative to the planet's true period of rotation in a process never before seen within planetary atmospheres.

Plain Language Summary

We observed Saturn's northern aurorae in the infrared using the Keck Observatory in Mauna Kea, Hawaii over the course of June, July and August of 2017. Using this data we investigate the motion of an ion, H_3^+, in the planet's upper atmosphere. This is done after first placing the data into four groups corresponding to the rotational phase of the planet's magnetic field. By doing so we are able to detect twin-vortex flows in the upper atmosphere of Saturn, consistent with theories that predict the presence of such a polar feature, thus providing direct evidence that Saturn's measured variable rotation rate is driven by these flows. These twin-vortex flows are ultimately responsible for the time differences relative to the planet's true rotation period observed throughout Saturn's planetary environment.

1 Introduction

An abiding mystery following Cassini's extended tour of Saturn is also one of the first questions the spacecraft raised about the planet: measurements showed that Saturn's day appeared to be 6 minutes longer at ∼10h 45m (Gurnett et al., 2005) than that measured by the Voyager 1 and 2 spacecraft (Kaiser et al., 1980). Since it is improbable that the interior of Saturn changed its rotation period over the course of only two decades, it was clear that somehow the magnetic fields above the planet were slipping relative to those generated deep within the interior (Stevenson, 2006). This mystery has remained unresolved despite nearly two decades of Cassini observations at Saturn.

First detected in the radio Saturn kilometric radiation and subsequently throughout the Cassini mission, evidence for a varying planetary rotation rate has been found in numerous parameters including: magnetospheric variations in the plasma (Gurnett et al., 2007), energetic neutrals (Paranicas et al., 2005) and the axisymmetric magnetic field (Giampieri et al., 2006), as well as ultraviolet (Nichols et al., 2008) and infrared (Badman et al., 2012) auroral emissions. The rotation rate also measurably drifts with time (Kurth et al., 2008), with two independent rates in the northern and southern hemispheres (Gurnett et al., 2009), linked to the changing season (Gurnett et al., 2010). These variations are propagated throughout the Saturnian environment by two large-scale planetary period current systems flowing between the ionosphere and magnetosphere (G. J. Hunt et al., 2014).

A wide range of models have been developed in order to explain the source of these planetary period currents with limited observational constraints to substantiate many of them. Some models place the source within the magnetosphere, caused by the Enceladus torus (Gurnett et al., 2007; Goldreich & Farmer, 2007; Burch et al., 2008), interactions with Titan (Winglee et al., 2013), or periodic latitudinal oscillations in the plasma sheet (Carbary et al., 2007). It is worth noting that magnetosphere-driven models are generally unable to robustly explain the distinction between the two independent periodicities observed in each polar region. Other models suggest that the source originates within Saturn's atmosphere, the result of changing ionospheric conductivity (Gurnett et al., 2007), flows in Saturn's stratosphere driving Hall drift (Smith, 2014), or the westward drift of ionospheric Rossby waves (Smith, 2018). Conversely, an alternative theory of how these currents are driven is that ions are forced to move through polar magnetic fields by collisions with rotating twin-vortex flows within Saturn's neutral polar thermosphere (Smith, 2006, 2011; Jia et al., 2012; Southwood & Cowley, 2014) – effectively a form of weather-driven aurora that is itself the result of neutral and ion winds flowing in the planet's upper atmospheric layers.

Tests of these theories using magnetospheric observations are difficult since both the magnetospheric currents and generated aurora are nearly identical whether they originate in the magnetosphere or the atmosphere. The only observational evidence for an atmospheric source comes from an apparent 1° modulation in the location of the planetary period auroral current layer, with maximum and minimum modulations occurring at southern magnetic phases of 270° and 90°, respectively, where local magnetic phases are analogous to magnetic longitude (G. J. Hunt et al., 2014). However, since the model predicting that these currents are driven by a thermospheric twin-cell vortex explicitly requires that the ionosphere flows in the opposite direction from other models, the motion of ions within the ionosphere provides a unique diagnostic of the source of planetary period currents (Smith, 2014).

Figure 1 shows these expected ion flows as would be seen by an observer at Earth with planetary dawn to the left and dusk to the right. In the case of a magnetospheric driver, at a noon northern magnetic phase of 0° (Ψ_{0°) as shown in Figure 1(a), ion-neutral collisions in the ionosphere lead to an anti-sunward flow (red-shifted) away from Earth-based observers over the central polar region with a return flow (blue-shifted) towards observers at lower latitudes. For an atmospheric driver at Ψ_{0°, seen in Figure 1(b), the neutral wind drives parallel plasma flow in the ionosphere, resulting in a sunward flow (blue-shifted) towards the observer over the polar region and an anti-sunward return flow (red-shifted) away from the observer at lower latitudes (G. J. Hunt et al., 2014; Jia et al., 2012; Southwood & Cowley, 2014; G. Hunt et al., 2015). In addition, these patterns rotate with phase at the measured period of the magnetic field oscillations.

2 Data Analysis

To test the thermospheric twin-cell vortex hypothesis, we used the Keck Observatory's Near Infrared Echelle Spectrograph (Keck-NIRSPEC) (McLean et al., 1998) to scan the auroral region in a manner similar to a study at Jupiter (Johnson et al., 2017), measuring emission from H_3^+ - a dominant molecular ion species in Saturn's ionosphere. The peak emission altitude of H_3^+ is at around 1,155 km above the atmospheric 1 bar level (T. S. Stallard et al., 2012) and is more generally found to exist between 1,000 to 2,000 km of the same altitudinal level (T. Stallard et al., 2010) which is, as demonstrated by Moore et al. (2010) and Shebanits et al. (2020), in the electrical dynamo region of the ionosphere. In a previous publication by T. S. Stallard et al. (2019), techniques were established to measure the line-of-sight velocity of H_3^+ emission lines on individual nights, providing a view of the varying ionospheric velocity in the Earth's reference frame. Similar work by O'Donoghue et al. (2016) and Chowdhury et al. (2019) have also provided insights into the H_3^+ aurorae at Saturn in recent years.

Here, we measure the ion velocities after mapping data into four rotational bins matching the phase (Ψ_N) of the magnetic field oscillation resulting from the rotating current system (Provan et al., 2018): Ψ_{0° (315° – 45°), Ψ_{90° (45° – 135°), Ψ_{180° (135° –

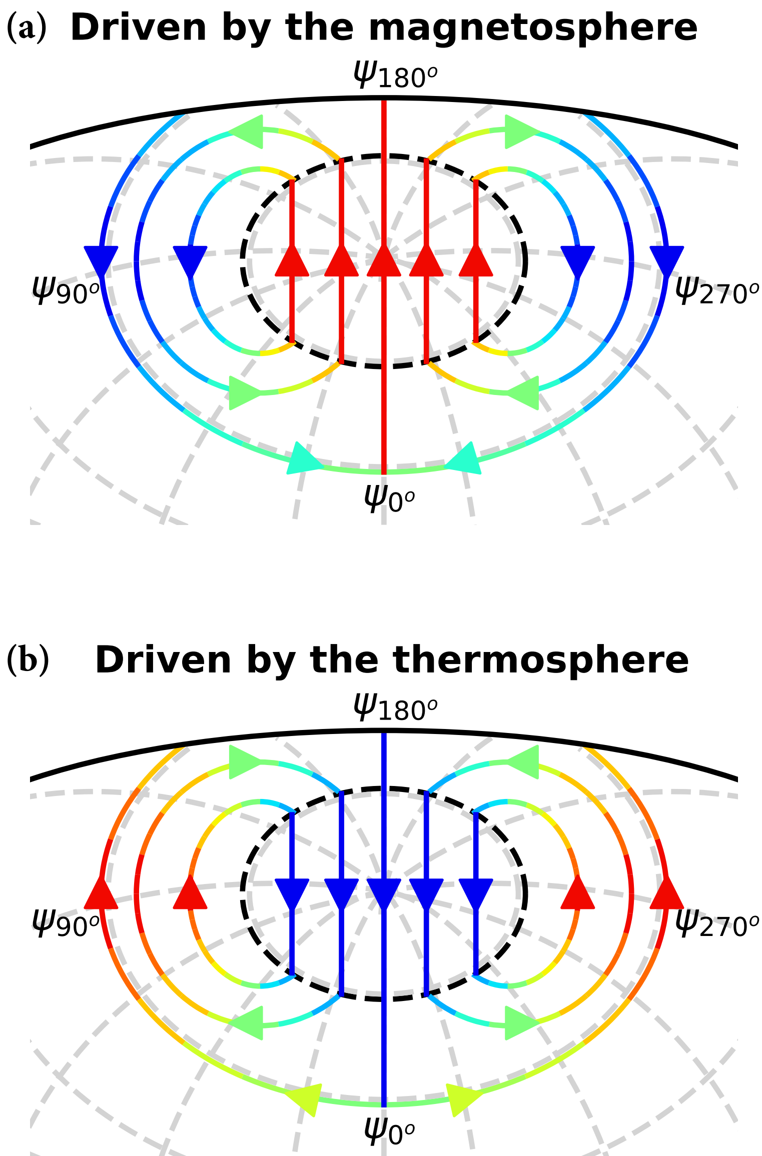

Figure 1. Predicted ion wind flows in Saturn's northern thermosphere (as observed from Earth) based on a magnetospheric (a) and thermospheric (b) source with planetary dawn on the left and dusk to the right. We adapt the predicted ion flows for a magnetospheric (G. J. Hunt et al., 2014) and atmospheric (G. Hunt et al., 2015) driver into what would be observed in the line-of-sight from Earth when the central meridian planetary phase (Ψ_N) is $0°$. Colors indicate in broad-scale the expected line-of-sight blue- and red-Doppler shifts. Magnetic fields are not shown here for the sake of the clarity, but can be found in the original works.

225°) and Ψ_{270° (225° – 315°), in order to reveal the underlying ion winds that are associated with the rotating current system. Tables S1 and S2 in the Supporting Information outline the corresponding night-by-night and quadrant-by-quadrant breakdown of spectra into the four aforementioned groupings of northern planetary magnetic phase.

Saturn's auroral currents and thus our line-of-sight velocity maps consist of subcorotational flows associated with the outer magnetosphere. Both the co-rotational flows and the outer magnetosphere are thought to be broadly fixed in local-time with the former rotating at the planetary period. In this work, we assume the local-time currents are the same no matter the rotational phase, while the rotating ion flows (containing both local-time and rotational phase components) are approximately equal in magnitude but opposite in direction for opposing phase quadrants. As such, subtracting the ion winds measured in two rotational phases in anti-phase (e.g. Ψ_{0° and Ψ_{180°) removes all the local-time fixed flows, thus isolating the rotating component of the flow which has subsequently doubled as a result of the subtraction; the same technique has previously been used with magnetospheric currents (G. J. Hunt et al., 2014). After dividing these data products by two in order to give an average velocity of rotational phase-associated ion flows, we are able to produce two difference maps of the ion winds ($\Psi_{0^\circ-180^\circ}$ and $\Psi_{90^\circ-270^\circ}$) at planetary phases that are perpendicular to one another.

Please refer to the Supporting Information for a more explicit account of the arithmetical considerations involved in this process.

3 Results

Figure 2(c) shows profile plots of the average intensity ($\Psi_{0^\circ+180^\circ}$) and the ion difference winds within the rotating phase ($\Psi_{0^\circ-180^\circ}$), computed as the means of the region delineated by dashed horizontal lines in Figure 2(a) and (b). This shows: blue shifted +0.5 km s^{-1} ion winds across the pole, inside (poleward of) the main auroral oval, well above the errors; a stagnant region close to the main auroral emission; and, a red-shifted -0.5 km s^{-1} ion wind along the flanks (at lower latitudes), equatorward of the main auroral emission. We would expect auroral intensity to be symmetric about the pole, but instead observe a brightening on the dusk side (right side) of the aurora; this indicates that an upward current in this region that is stronger at dusk may be affected by local-time ion winds. Figure 2(f) shows the perpendicular average intensity ($\Psi_{90^\circ+270^\circ}$) and ion difference velocity ($\Psi_{90^\circ-270^\circ}$). These are more symmetric in intensity but include a brightening near noon similar to a local-time cusp brightening observed in previous intensities (Badman et al., 2011); the velocities are harder to interpret until placed in the context of Figure 3.

In Figure 3 we combine the two perpendicular line-of-sight ion wind difference maps from Figure 2(b) and (e) – $\Psi_{0^\circ-180^\circ}$ flowing from midnight (top) to noon (bottom) and $\Psi_{90^\circ-270^\circ}$ flowing from dusk (right) to dawn (left) – into a two-dimensional map of ionospheric flows as seen from Earth at a noon rotational phase of Ψ_{0°, enabling comparison with the schematics presented in Figure 1. This clearly shows a strong blue-shifted flow over the pole, and a red-shifted return flow along the dawn side of the lower latitude sub-auroral region, as well as some evidence for a second return flow on the dusk side of the polar region. This accords well with models that make use of a thermospheric driver to explain the observed behavior in Saturn's polar auroral regions (Smith, 2011).

Ions across the pole can only flow towards us in this configuration if they are blown by a strong coincident thermospheric neutral wind, as other sources would cause the flow to move away from us (Smith, 2014). Magnetospheric sources of the planetary period oscillations cannot explain the observed flows, as the magnetospheric currents would drive ions to flow away from the observer over the pole, irrespective of the sources of this os-

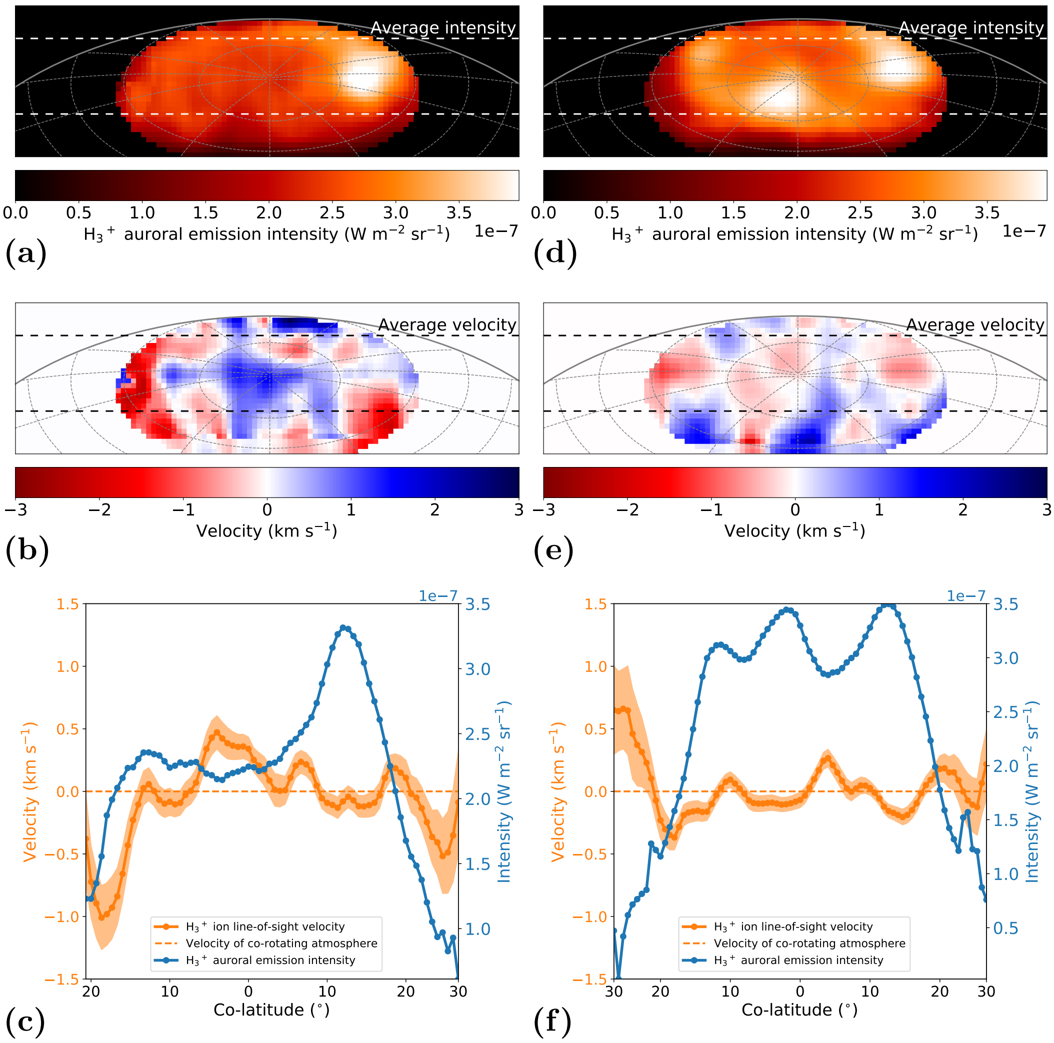

Figure 2. Auroral emission intensity maps and ion wind velocity difference maps for $\Psi_{0^\circ-180^\circ}$ and $\Psi_{90^\circ-270^\circ}$ with planetary dawn to the left and dusk to the right. We make use of the individual emission intensity and ion line-of-sight velocity maps for each of the four quadrant groupings of rotational phase (shown in Figure S1 in the Supplementary Information) to produce average emission intensity maps for Ψ_{0° and Ψ_{180° ($\Psi_{0^\circ+180^\circ}$), shown in panel (a), and for Ψ_{90° and Ψ_{270° ($\Psi_{90^\circ+270^\circ}$), shown in panel (d). We also subtract the observed ion velocity at Ψ_{180° from Ψ_{0° and the velocity at Ψ_{270° from Ψ_{90° to create ion wind difference maps for $\Psi_{0^\circ-180^\circ}$ and $\Psi_{90^\circ-270^\circ}$ displayed in panels (b) and (e), respectively. Overall H_3^+ emission structures shown in (a) and (d) reveal a bright spot on the dusk of $\Psi_{0^\circ+180^\circ}$ and broadly symmetric emission in $\Psi_{90^\circ+270^\circ}$. The line-of-sight velocity difference maps, seen in (b) and (e), show clear structures with $\Psi_{0^\circ-180^\circ}$ dominated by a blue-shift over the pole and red-shift on the flanks, and $\Psi_{90^\circ-270^\circ}$ highlighting more complexity. The average emission intensities and ion winds for each (taken from between the dotted horizontal lines in the maps) are illustrated in (c) and (f). These show intensities of $\sim$3.5 W m^{-2} sr^{-1} across the auroral region and ion wind difference flows up to $\sim \pm 0.5$ km s^{-1}, well above the errors.

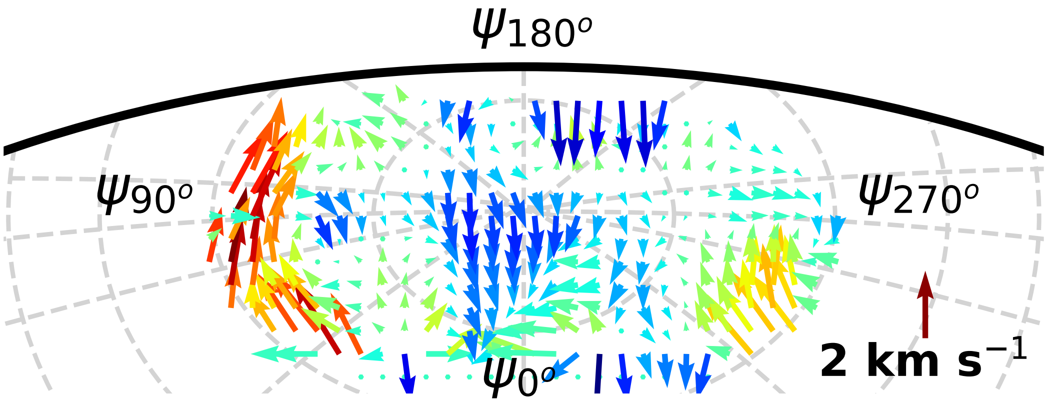

Figure 3. Our combined observed ion flows as seen from Earth with Saturnian dawn to the left and dusk to the right. Velocities are again shown at a noon magnetic phase of Ψ_{0°, as in Figure 1. The vectors represent flows from Figure 2(b) and (e), with blue-shifted $\Psi_{0^\circ-180^\circ}$ flowing from midnight to midday (top to bottom), and $\Psi_{90^\circ-270^\circ}$ flowing from dusk to dawn (right to left). The magnitude of the arrows is scaled with velocity up to ∼2.4 km s^{-1}, and the blue-to-red color represents the magnitude in the $\Psi_{0^\circ-180^\circ}$ direction. Please note that the magnitudes of the arrows shown here correspond exactly with velocities presented in Figure 2(b) and (e). A clear blue-shift across the pole and red-shift along the lower latitude flanks matches well with Figure 1(b), making it consistent with a thermospheric origin for the ion winds. It is as yet unclear why the dawn (left) side vortex is more intense than the much weaker corresponding dusk (right) side vortex. One possibility may be that the current emerging from the dawn side vortex (Ψ_{90°) is higher than the one which emerges from the dusk side vortex (Ψ_{270°). Furthermore, it is not unreasonable to surmise that the dawn side vortex will weaken as it rotates into noon (Ψ_{0°) and through to the dusk side while the dusk side vortex will strengthen as it rotates into midnight (Ψ_{180°) through to the dawn side.

cillation (Gurnett et al., 2007; Goldreich & Farmer, 2007; Burch et al., 2008; Winglee et al., 2013; Carbary et al., 2007).

4 Discussion & Conclusions

Having excluded all other theories of how the planetary period current system is generated, our measurements of a sunward (midnight to noon) flow across the pole in the northern ionosphere provides direct evidence that the variable measured rotation rate of Saturn is produced by a source within the planet's atmosphere. The observed flows match very well with predicted flows from models using a previously undetected twin-vortex within the thermosphere of the planet, driving currents out into the magnetosphere and producing a radio pulse. The temporal variations in rotational period seen within the radio emission, and throughout Saturn's magnetosphere, must result from long-term localised variations in the rotation speed of this atmospheric twin-vortex.

The atmospheric vortex model proposed by (Jia et al., 2012) for a single source in one hemisphere and for dual sources in two hemispheres (Jia & Kivelson, 2012), which successfully reproduced many of the observed magnetospheric periodicities, invoked vortical flows in the ionosphere with speeds ranging between 0.3 and 3 km s^{-1}. Unfortunately, this does not enable us to conclude anything substantial relating to the altitudinal location of the driving vortices because not enough is known about the dynamics of the thermosphere or indeed the underlying neutral atmospheric weather that drives this ion flow and the resultant magnetospheric current system. Models of how thermospheric flows might generate these ion winds resulted in a comparable twin-cell flow by placing a heat source located at auroral latitudes between Ψ_{30° and Ψ_{210° (Smith, 2011). This places the source of heating close to the region of brightest aurora, perhaps hinting that these flows may be self-sustaining. However, such modelling predicts much smaller ion winds than those we observe.

Subsequent modelling predicted significant heating when driving flows at the magnitude observed here. Future observations should constrain the neutral flows and how they drive this ionospheric twin-cell vortex, and help resolve whether localised heating places the thermal source of this twin-cell in the thermosphere itself, or if it is driven by other deeper atmospheric processes (Smith, 2014). Additionally, with favorable viewing geometries, observations of the southern hemisphere will also allow the other half of this picture to be pieced together.

Our findings provide direct evidence that it is the thermosphere driving the system and helps to answer the long-standing question of why the period of magnetic field oscillations resulting from the current system varies at Saturn. We have also presented the first known example of weather-driven aurora as neutral winds in the thermosphere drive the currents which go on to exert forces in the magnetosphere. If atmospheric weather at Saturn can drive intensity perturbations in auroral emissions then it stands to highlight the potential importance of giant planets possessing significantly strong feedback systems whereby neutral atmospheres can drive the magnetospheres; a major factor in the context of the Saturn field-aligned current.

Recent observations at Earth have evidenced non-auroral forcing of the equatorial magnetospheric regions, as neutral atmospheric dynamics appear to drive ionospheric flows at altitudes of 600 km above the surface (Immel et al., 2021). A similar example of equatorial neutral driving is suggested for the azimuthal magnetic field structures observed in Saturn's equatorial regions, where tropospheric winds have been evoked to explain magnetic field variations (Khurana et al., 2018; Agiwal et al., 2021). Both Uranus and Neptune have highly inclined magnetic poles, placing them in these same equatorial regions, suggesting even modest flows similar to either Earth or Saturn could drive dramatic new weather-driven aurora at those planets.

Observations have shown that planets close to their star experience intense atmospheric heating, resulting in strong neutral winds. For example, HD 189733b is a Hot Jupiter that has a lower atmosphere super-rotating at 3 km s^{-1} that becomes a vertical 40 km s^{-1} neutral outflow at the top of the upper atmosphere (Seidel et al., 2020). These authors evoke the super-rotation of ions in the upper atmosphere across the magnetic field to explain this outward atmospheric flow. Such an intense neutral wind interaction is vastly stronger than the ion winds observed at Saturn, and would result in commensurately stronger auroral currents. These flows may help explain the detection of aurora (Pineda, 2020) from a proposed close-in Hot Super-Earth planet GJ 1151b (Mahadevan et al., 2021), the production of which does not match with present theories of auroral generation at these worlds, perhaps indicating that close-in planetary aurora are dominated by atmospherically driven interactions, rather than currents from the surrounding space environment.

While planetary radio measurements remain a powerful tool for determining planetary rotation rates, interpreting such measurements requires detailed knowledge of ion-neutral coupling in the ionosphere-thermosphere. This work provides observational evidence to support such arguments. As such, ion wind measurements could be used to explore the impact of atmospheric effects on planetary periods, particularly in cases where there exists an axisymmetric planetary magnetic field and a system with a tilted dipole masking the effects of such setups, both within our own solar system and farther afield.

Acknowledgments

This work was supported by a NASA Keck PI Data Award, administered by the NASA Exoplanet Science Institute. Data presented herein were obtained at the W. M. Keck Observatory from telescope time allocated to the National Aeronautics and Space Administration through the agency's scientific partnership with the California Institute of Technology and the University of California. All data used in the study are publicly available on the Keck Observatory Archive (KOA) [https://www2.keck.hawaii.edu/koa/public/koa.php]. The Observatory was made possible by the generous financial support of the W. M. Keck Foundation. We wish to place on record our recognition of the highly significant reverence and cultural role that the summit of Mauna Kea has always had within the indigenous Hawaiian community. We consider ourselves incredibly fortunate to have had the opportunity to take our observations from within this sacred vicinity.

Open Research: Keck-NIRSPEC data used in this study are publicly available on the Keck Observatory Archive (KOA) [https://www2.keck.hawaii.edu/koa/public/koa.php]. Similarly, the planetary period oscillation phases obtained from NASA Cassini magnetic field data that have been employed in this study are available from the University of Leicester Research Archive [http://hdl.handle.net/2381/42436]. Further details are outlined in Provan et al. (2018).

MNC and EMT were supported by UK Science and Technology Facilities Council (STFC) Studentship Grants ST/N504117/1 and ST/R000816/1, respectively. TSS, GP, GJH, and SVB were all respectively supported by UK STFC Consolidated Grants ST/N000749/1, ST/N000749/1, ST/S000364/1, and ST/V000748/1. SVB was also supported by a UK STFC Ernest Rutherford Fellowship ST/M005534/1. KHB was supported by a Keck Principal Investigator Data Award and the research was carried out at the Jet Propulsion Laboratory, California Institute of Technology, under a contract with the National Aeronautics and Space Administration (80NM0018D0004). HM was supported by a European Research Council Consolidator Grant (under the European Union's Horizon 2020 research and innovation programme, grant agreement no. 723890). LM was supported by a National Aeronautics and Space Administration grant, no. 80NSSC19K0546 issued through the Solar System Workings Program. And, last but not least, JOD was supported by a Japan Aerospace Exploration Agency (JAXA) International Top Young Fellowship.

Author contributions (CRediT) - Mohammad Nahid Chowdhury: Data Curation, Formal Analysis, Methodology, Software, Visualization, Writing - Original Draft, Writing - Review & Edit; Thomas S. Stallard: Conceptualization, Data Curation, Formal Analysis, Funding Acquisition, Investigation, Methodology, Project Administration, Resources, Software, Supervision, Validation, Visualization, Writing - Original Draft, Writing - Review & Edit; Kevin H. Baines: Funding Acquisition, Project Administration, Writing - Review & Edit; Gabrielle Provan: Data Curation, Methodology, Resources, Software, Writing - Review & Edit; Henrik Melin: Conceptualization, Data Curation, Methodology, Resources, Software, Writing - Review & Edit; Gregory J. Hunt: Conceptualization, Methodology, Writing - Review & Edit; Luke Moore: Conceptualization, Writing - Review & Edit; James O'Donoghue: Conceptualization, Visualization, Writing - Review & Edit; Emma M. Thomas: Conceptualization, Software; Ruoyan Wang: Conceptualization, Software; Steve Miller: Conceptualization, Methodology, Validation, Writing - Review & Edit; Sarah V. Badman: Conceptualization, Validation, Visualization, Writing - Review & Edit.

References

Agiwal, O., Cao, H., Cowley, S., Dougherty, M., . Hunt, G., Müller-Wodarg, I., & Achilleos, N. (2021). Constraining the temporal variability of neutral winds in saturn's low-latitude ionosphere using magnetic field measurements. *Journal of Geophysical Research: Planets*, *126*(2), e2020JE006578.

Badman, S. V., Andrews, D. J., Cowley, S., Lamy, L., Provan, G., Tao, C., ... others (2012). Rotational modulation and local time dependence of saturn's infrared h_3^+ auroral intensity. *Journal of Geophysical Research: Space Physics*, *117*(A9).

Badman, S. V., Tao, C., Grocott, A., Kasahara, S., Melin, H., Brown, R. H., ... Stallard, T. (2011). Cassini vims observations of latitudinal and hemispheric variations in saturn's infrared auroral intensity. *Icarus*, *216*(2), 367–375.

Burch, J., Goldstein, J., Mokashi, P., Lewis, W., Paty, C., Young, D., ... André, N. (2008). On the cause of saturn's plasma periodicity. *Geophysical research letters*, *35*(14).

Carbary, J., Mitchell, D., Krimigis, S., Hamilton, D., & Krupp, N. (2007). Spin-period effects in magnetospheres with no axial tilt. *Geophysical research letters*, *34*(18).

Chowdhury, M., Stallard, T., Melin, H., & Johnson, R. (2019). Exploring key characteristics in saturn's infrared auroral emissions using vlt-crires: Intensities, ion line-of-sight velocities, and rotational temperatures. *Geophysical Research Letters*, *46*(13), 7137–7146.

Giampieri, G., Dougherty, M. K., Smith, E., & Russell, C. T. (2006). A regular period for saturn's magnetic field that may track its internal rotation. *Nature*, *441*(7089), 62–64.

Goldreich, P., & Farmer, A. J. (2007). Spontaneous axisymmetry breaking of the external magnetic field at saturn. *Journal of Geophysical Research: Space Physics*, *112*(A5).

Gurnett, D., Groene, J., Persoon, A., Menietti, J., Ye, S.-Y., Kurth, W., ... Lecacheux, A. (2010). The reversal of the rotational modulation rates of the north and south components of saturn kilometric radiation near equinox. *Geophysical Research Letters*, *37*(24).

Gurnett, D., Kurth, W., Hospodarsky, G., Persoon, A., Averkamp, T., Cecconi, B., ... others (2005). Radio and plasma wave observations at saturn from cassini's approach and first orbit. *Science*, *307*(5713), 1255–1259.

Gurnett, D., Lecacheux, A., Kurth, W., Persoon, A., Groene, J., Lamy, L., … Carbary, J. (2009). Discovery of a north-south asymmetry in saturn's radio rotation period. *Geophysical Research Letters*, *36*(16).

Gurnett, D., Persoon, A., Kurth, W., Groene, J., Averkamp, T., Dougherty, M., & Southwood, D. (2007). The variable rotation period of the inner region of saturn's plasma disk. *science*, *316*(5823), 442–445.

Hunt, G., Cowley, S., Provan, G., Bunce, E., Alexeev, I., Belenkaya, E., … Coates, A. (2015). Field-aligned currents in saturn's northern nightside magnetosphere: Evidence for interhemispheric current flow associated with planetary period oscillations. *Journal of Geophysical Research: Space Physics*, *120*(9), 7552–7584.

Hunt, G. J., Cowley, S. W., Provan, G., Bunce, E. J., Alexeev, I. I., Belenkaya, E. S., … Coates, A. J. (2014). Field-aligned currents in saturn's southern nightside magnetosphere: Subcorotation and planetary period oscillation components. *Journal of Geophysical Research: Space Physics*, *119*(12), 9847–9899.

Immel, T., Harding, B., Heelis, R., Maute, A., Forbes, J. M., England, S., … others (2021). Control of ionospheric plasma velocities by thermospheric winds.

Jia, X., & Kivelson, M. G. (2012). Driving saturn's magnetospheric periodicities from the upper atmosphere/ionosphere: Magnetotail response to dual sources. *Journal of Geophysical Research: Space Physics*, *117*(A11).

Jia, X., Kivelson, M. G., & Gombosi, T. I. (2012). Driving saturn's magnetospheric periodicities from the upper atmosphere/ionosphere. *Journal of Geophysical Research: Space Physics*, *117*(A4).

Johnson, R. E., Stallard, T. S., Melin, H., Nichols, J. D., & Cowley, S. W. (2017). Jupiter's polar ionospheric flows: High resolution mapping of spectral intensity and line-of-sight velocity of h_3^+ ions. *Journal of Geophysical Research: Space Physics*, *122*(7), 7599–7618.

Kaiser, M. L., Desch, M. D., Warwick, J. W., & Pearce, J. B. (1980). Voyager detection of nonthermal radio emission from saturn. *Science*, *209*(4462), 1238–1240.

Khurana, K., Dougherty, M., Provan, G., Hunt, G., Kivelson, M., Cowley, S., … Russell, C. (2018). Discovery of atmospheric-wind-driven electric currents in saturn's magnetosphere in the gap between saturn and its rings. *Geophysical Research Letters*, *45*(19), 10–068.

Kurth, W., Averkamp, T., Gurnett, D., Groene, J., & Lecacheux, A. (2008). An update to a saturnian longitude system based on kilometric radio emissions. *Journal of Geophysical Research: Space Physics*, *113*(A5).

Mahadevan, S., Stefánsson, G., Robertson, P., Terrien, R. C., Ninan, J. P., Holcomb, R. J., … others (2021). The habitable-zone planet finder detects a terrestrial-mass planet candidate closely orbiting gliese 1151: The likely source of coherent low-frequency radio emission from an inactive star. *arXiv preprint arXiv:2102.02233*.

McLean, I. S., Becklin, E. E., Bendiksen, O., Brims, G., Canfield, J., Figer, D. F., … others (1998). Design and development of nirspec: a near-infrared echelle spectrograph for the keck ii telescope. In *Infrared astronomical instrumentation* (Vol. 3354, pp. 566–578).

Moore, L., Mueller-Wodarg, I., Galand, M., Kliore, A., & Mendillo, M. (2010). Latitudinal variations in saturn's ionosphere: Cassini measurements and model comparisons. *Journal of Geophysical Research: Space Physics*, *115*(A11).

Nichols, J. D., Clarke, J., Cowley, S., Duval, J., Farmer, A., Gérard, J.-C., … Wannawichian, S. (2008). Oscillation of saturn's southern auroral oval. *Journal of Geophysical Research: Space Physics*, *113*(A11).

O'Donoghue, J., Melin, H., Stallard, T. S., Provan, G., Moore, L., Badman, S. V., … Blake, J. S. (2016). Ground-based observations of saturn's auroral ionosphere over three days: Trends in h_3^+ temperature, density and emission with

saturn local time and planetary period oscillation. *Icarus*, *263*, 44–55.
Paranicas, C., Mitchell, D., Roelof, E., Brandt, P., Williams, D., Krimigis, S., & Mauk, B. (2005). Periodic intensity variations in global ena images of saturn. *Geophysical Research Letters*, *32*(21).
Pineda, J. S. (2020). Stellar radio aurorae signal planetary systems. *Nature Astronomy*, *4*(6), 562–563.
Provan, G., Cowley, S., Bradley, T., Bunce, E., Hunt, G., & Dougherty, M. (2018). Planetary period oscillations in saturn's magnetosphere: Cassini magnetic field observations over the northern summer solstice interval. *Journal of Geophysical Research: Space Physics*, *123*(5), 3859–3899.
Seidel, J., Ehrenreich, D., Pino, L., Bourrier, V., Lavie, B., Allart, R., … Lovis, C. (2020). Wind of change: retrieving exoplanet atmospheric winds from high-resolution spectroscopy. *Astronomy & Astrophysics*, *633*, A86.
Shebanits, O., Hadid, L., Cao, H., Morooka, M., Hunt, G., Dougherty, M., … Müller-Wodarg, I. (2020). Saturn's near-equatorial ionospheric conductivities from in situ measurements. *Scientific reports*, *10*(1), 1–13.
Smith, C. (2006). Periodic modulation of gas giant magnetospheres by the neutral upper atmosphere. In *Annales geophysicae* (Vol. 24, pp. 2709–2717).
Smith, C. (2011). A saturnian cam current system driven by asymmetric thermospheric heating. *Monthly Notices of the Royal Astronomical Society*, *410*(4), 2315–2328.
Smith, C. (2014). On the nature and location of the proposed twin vortex systems in saturn's polar upper atmosphere. *Journal of Geophysical Research: Space Physics*, *119*(7), 5964–5977.
Smith, C. (2018). Interaction of saturn's dual rotation periods. *Icarus*, *302*, 330–342.
Southwood, D., & Cowley, S. W. H. (2014). The origin of saturn's magnetic periodicities: Northern and southern current systems. *Journal of Geophysical Research: Space Physics*, *119*(3), 1563–1571.
Stallard, T., Melin, H., Cowley, S. W., Miller, S., & Lystrup, M. B. (2010). Location and magnetospheric mapping of saturn's mid-latitude infrared auroral oval. *The Astrophysical Journal Letters*, *722*(1), L85.
Stallard, T. S., Baines, K. H., Melin, H., Bradley, T. J., Moore, L., O'Donoghue, J., … others (2019). Local-time averaged maps of h_3^+ emission, temperature and ion winds. *Philosophical Transactions of the Royal Society A*, *377*(2154), 20180405.
Stallard, T. S., Melin, H., Miller, S., Badman, S. V., Brown, R. H., & Baines, K. H. (2012). Peak emission altitude of saturn's h3+ aurora. *Geophysical research letters*, *39*(15).
Stevenson, D. J. (2006). A new spin on saturn. *Nature*, *441*(7089), 34–35.
Winglee, R., Kidder, A., Harnett, E., Ifland, N., Paty, C., & Snowden, D. (2013). Generation of periodic signatures at saturn through titan's interaction with the centrifugal interchange instability. *Journal of Geophysical Research: Space Physics*, *118*(7), 4253–4269.